PHILOSOPHICAL TRANSACTIONS OF THE ROYAL SOCIETY A
MATHEMATICAL, PHYSICAL & ENGINEERING SCIENCES

Eddy Diffusion of Momentum, Water Vapour, and Heat near the Ground

N. E. Rider

Phil. Trans. R. Soc. Lond. A 1954 **246**, 481-501
doi: 10.1098/rsta.1954.0006

EDDY DIFFUSION OF MOMENTUM, WATER VAPOUR, AND HEAT NEAR THE GROUND

By N. E. RIDER

Meteorological Office, London, and School of Agriculture, University of Cambridge

(*Communicated by O. G. Sutton, F.R.S.—Received* 14 *November* 1953—*Revised* 23 *December* 1953—*Read* 25 *March* 1954)

CONTENTS

An account is given of an experimental study of the factors which control the vertical turbulent transport of momentum, water vapour, and heat in the first 2 m of air above a short grass surface. The results of fifty-one observations, each of which extended over 30 min, are presented. Measurements were made of the vertical profiles of wind speed, temperature and humidity, and of the rate of evaporation and the aerodynamic drag of the surface. Measurement of the heat-balance components was also attempted. On any one occasion it was not generally possible to observe all the desired quantities.

It is found that the wind speed and temperature profiles always have the same form, and that this form is shared on the majority of occasions by the humidity profile. The profiles depart from the logarithmic form found in adiabatic conditions in the manner suggested by Deacon. In near adiabatic conditions as defined by small numerical values of the Richardson number the established laboratory law relating the surface drag to the fluid velocity over a rough surface in turbulent flow is found to hold over the site and a value is deduced for von Kármán's constant. In conditions other than adiabatic it is shown that the explicit wind profile law suggested by Deacon holds in unstable but not in stable conditions. In the latter conditions equations proposed by Rossby & Montgomery and by Holtzman are found to represent the observations with reasonable precision. The friction coefficient of the surface is computed and found to be independent of wind speed but to increase in value in unstable conditions. Values of the eddy diffusivity for momentum, water vapour and heat are obtained on a direct observational basis from the expressions from which the diffusivities are normally defined, and it is found that the diffusivities for momentum and vapour are identical over the range of stability experienced. The magnitude of the diffusivity for heat often appears to be approximately the same as that for momentum or vapour, but exceptions occur when it is much larger than the other two. The exceptions do not appear to be related to stability.

1. Introduction

Eddy diffusion is of fundamental importance in meteorology, particularly in relation to the microclimatic region. Since the first recognition of the transfer of momentum, matter and heat in the atmosphere by turbulence interest has largely centred on the magnitude of the diffusivities, their dependence on various physical processes and their relationship to one another. A considerable amount of information is now available from wind-tunnel studies in the laboratory of factors such as aerodynamic drag and evaporation, but, primarily as a result of the difficulties introduced by the nature of natural surfaces and absence of control, investigations in the open have tended to lag behind. In treating diffusion problems in the atmosphere it has been the usual practice to assume the equality of at least two of the diffusivities, an assumption that has often led to the construction of formulae in good agreement with observation. A notable contribution was made by Pasquill (1949*a*), who demonstrated the equality of the eddy diffusivities for momentum and vapour in neutral conditions by assuming the validity (which he later confirmed (1950)) of the laboratory law relating the drag exerted on a surface to the fluid velocity above the surface in the lowest layers of the atmosphere. He showed further that in unstable conditions, but not in stable conditions, his observed values of the eddy diffusivity for vapour were in good agreement with values of the eddy diffusivity for momentum when the latter were calculated on the basis of Deacon's (1949) generalized wind-profile law. He questioned the normally accepted identity of the diffusivities for heat and vapour in all conditions of stability. Rider & Robinson (1951) undertook a similar study but concluded that it was unlikely that the diffusivities for heat and vapour were not equal in all conditions of stability.

The present work was undertaken to take advantage of a technique for the measurement of the drag exerted on a natural surface by the wind from which values of the eddy diffusivity for momentum could be obtained on a direct observational basis, so permitting a comparison to be made with the diffusivities for water vapour and heat determined simultaneously over the same site. The explicit validity of wind-profile laws can also be studied once this measurement has been made in a range of stability conditions.

2. The site and observations

Observations were made on the airfield at Cardington. A circular area of approximately 250 m diameter was kept mown to a grass length of 2 to 3 cm, and from the centre of this area to a distance of 300 m in an arc of 200° centred about south-east there were no obstacles to the flow of air. Figure 1 shows a plan of the site. Observations were made in the period July to November 1952 when wind directions within this arc were experienced. Generally it was not possible to observe all the appropriate quantities on every occasion, and the observations have been divided into two series. The first series of observations, nos. 1 to 26, contains temperature and wind-speed profiles together with a determination of the drag. In the second series, observations nos. 27 to 51, measurement of the humidity profile together with a direct determination of the rate of natural evaporation was added. Further, in this second series, measurement of the gain or loss of heat in the ground and of the short- and long-wave radiation components was attempted when clear sky conditions prevailed. During a few of the observations no measurement of the surface drag was possible; this occurred when the wind direction was unusually variable.

Air temperature and humidity profiles were measured with an installation of dry and wet aspirated thermo-electric thermometers mounted on a mast specially constructed for the purpose. Psychrometer units were mounted at 25, 37·5, 50, 100, 150 and 200 cm. The constructional details of the apparatus have been given by Pasquill (1949*b*), but the method of wiring and switching was changed so that the dry-bulb temperature at 2 m was found to 0·1° F with reference to melting ice and the dry-bulb temperatures at the other five heights were found as differences to 0·01° F from the 2 m thermometer. Wet-bulb depressions were read to 0·01° F. In the 30 min observation period readings were taken in two 12 min periods separated by an interval of 4 min. In the working time of 24 min a determination of the temperature and the wet-bulb depression at each height was obtained every minute, the profiles then being constructed from the means of the individual observations. Wind-speed measurements were made with sensitive cup anemometers similar to those described by Sheppard (1940). Eight were exposed at heights between 15 cm and 2 m. It was not possible

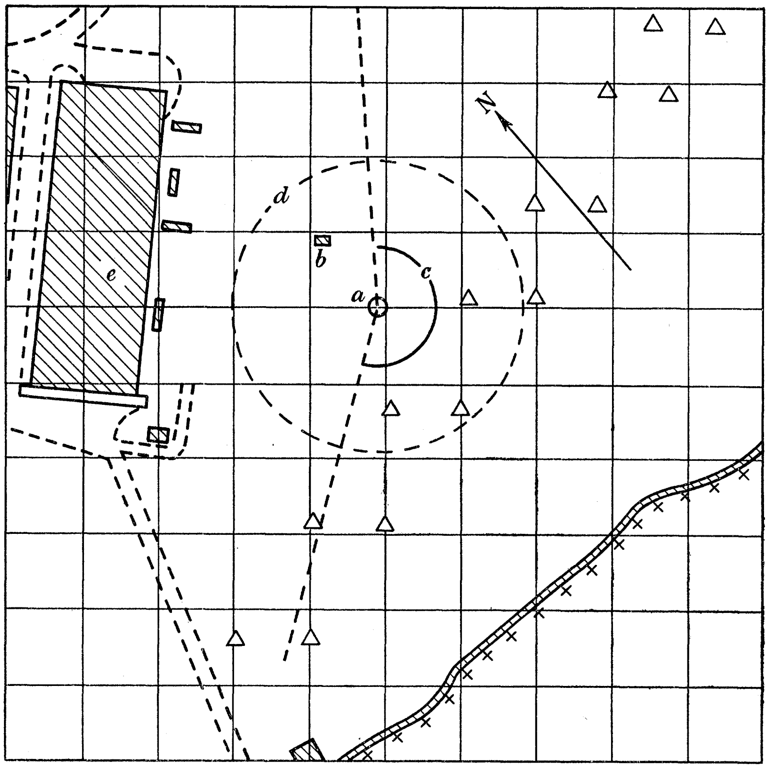

FIGURE 1. Plan of the experimental site on a 65 m grid. *a*, position of the instruments; *b*, the mobile laboratory; *c*, the arc from within which winds blew to the instruments when observations were made; *d*, a 250 m diameter circle; *e*, a building having a height of 57 m. Δ indicates the limits of a temporary grass runway; ⁝⁝⁝ tarmac areas; ▭, an open drain; × × ×, an open wire fence.

to mount all on one mast, so that some scatter was expected in the results owing to the small-scale undulations of the natural surface, the height of each anemometer being set with reference to the ground at the foot of its mounting. The anemometers were allowed to run for two periods of 10 min separated by an interval of 6 min with frequent interchanges of instruments.

The apparatus used for the measurement of the surface drag is shown in figure 2 and was similar in principle to that used by Pasquill (1950). Six sets of apparatus were available and each consisted of two vertical-sided aluminium pans having diameters of 18 and 20 in. respectively. The smaller, slightly more shallow, pan was provided with a false bottom to carry a sample of the turf surface and had two rigid links at opposite ends of a diameter. One link supported a rigid brass clamp, the other enabled a 30 in. light Duralumin arm with an air damping plate at its centre and a syphon-type pen at its far end, to be attached rigidly to the smaller pan. The smaller pan floated in water contained in the larger pan, and

PHILOSOPHICAL TRANSACTIONS OF THE ROYAL SOCIETY A MATHEMATICAL, PHYSICAL & ENGINEERING SCIENCES

the pen rested on a chart over a drum mounted on a horizontal axis at right angles to the axis of symmetry of the apparatus, the drum being driven by a synchronous motor to rotate once in 30 min. Control of the movement of the inner pan in the horizontal was obtained by a vertically mounted phosphor-bronze suspension held firmly to the outer side of the larger pan. The suspension was provided with means for tensioning and zero adjustment and various suspensions could be used as required. The brass clamp attached to the smaller pan provided the means to attach the latter to the centre of the suspension. Calibration of the plates used on any day was performed before and after the day's observations, the suspensions used providing a range of sensitivity from approximately 1 to 3 cm dyne^{-1} cm^{-2}

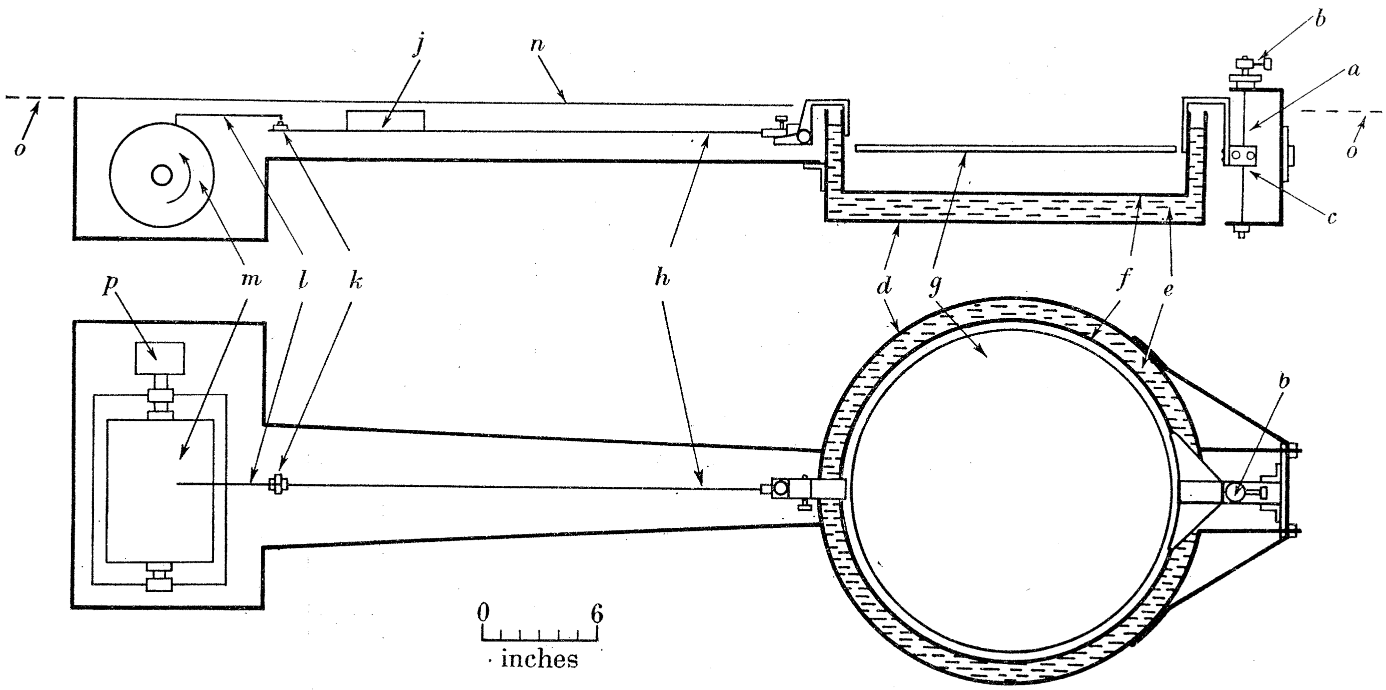

FIGURE 2. Section and plan of the drag plate apparatus. *a*, phosphor-bronze suspension; *b*, torsion head; *c*, brass clamp; *d*, outer pan; *e*, water; *f*, inner pan; *g*, false bottom to carry surface sample; *h*, light arm with damping plate, *j*, and support for syphon-type pen, *k*; *l*, pen; *m*, chart drum; *n*, transparent covers; *o*, ground level; *p*, synchronous motor.

of exposed sample area on the chart. In the field sufficient soil was removed to allow the outer pan to be inserted to below the level of its top rim. A box containing the pen arm and the drum together with its driving mechanism was also sunk below surface level and covered with a Perspex lid. *In situ* the only parts of the apparatus projecting above ground level were the top of the torsion head and the links from the inner pan to the suspension and pen arm. These projections were within the grass length and the links were screened by faired plates. The six sets of apparatus were arranged with their axes of symmetry as tangents to a circle of about 8 m radius spaced 40° apart over the arc from which unobstructed winds were available. A light bi-directional vane of the type used by Best (1935) was mounted at the centre of this circle, and during an observation the two plates over and between which the wind was expected to blow to the vane were allowed to record. The layout of the drag plates and other apparatus on the experimental site is shown in figure 3. Covers enabled the zero positions to be obtained, and the procedure was to take a 30 min trace from two plates of which the first and last minutes were occupied by zero lines. Computations were based on the parts of the records occupying the periods 2 to 12 min and 18 to 28 min, the two periods of anemometer operation. Temperature and humidity measurements were made in the periods 1 to 13 min and 17 to 29 min. Four 3 min traces were provided by the vane, two in each period of the drag-plate operation. A planimeter was used to determine the force per unit area of exposed turf sample from the drag-plate records, and this (in association with the wind-direction records which enabled the angle between the axes of symmetry of the apparatus and the mean wind to be obtained) provided

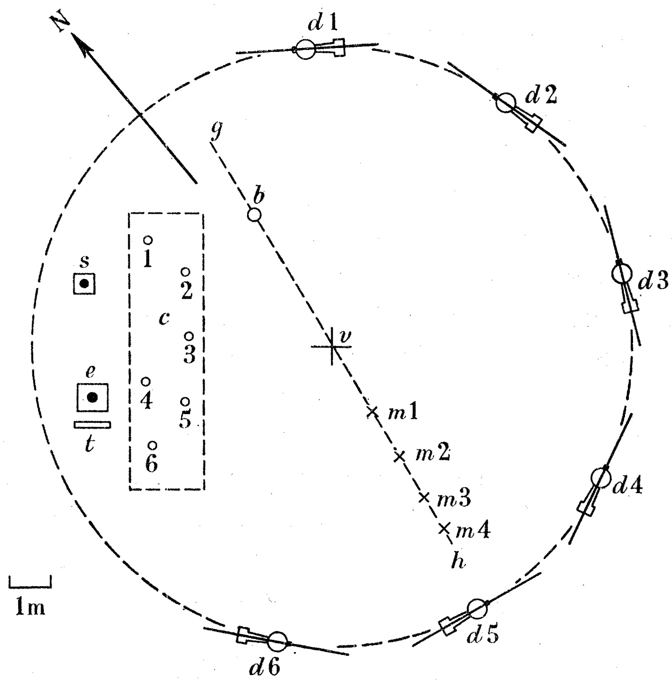

FIGURE 3. Diagram of the lay-out of the apparatus at position *a* of figure 1. *b*, the temperature and humidity profile mast; *c*, the area in which the evaporimeters were exposed; *d*1, ..., *d*6, the drag plate positions; *e*, the earth thermometer; *m*1, ..., *m*4, the anemometer masts; *s*, the solarimeter; *t*, the spirit in glass thermometer; *v*, the bi-directional vane. The profile mast and anemometer masts were moved as necessary to place the line *gh* approximately across wind.

a value for the mean drag. It soon became apparent that the values of the surface drag provided by each plate were not the same; they differed by as much as 30 %. This is not surprising when it is remembered that, as well as the difficulty of choosing and extracting two samples of the surface which were identical aerodynamically and were both typical of the site as a whole, the level of the inner pans had to be adjusted to expose the samples at their natural levels. This was a great difficulty in practice, and for this reason the value of the surface drag given for any one observation may be considerably in error. By re-levelling the inner pans between each observation and changing the surface samples every few days an attempt was made to produce a result which would at least have statistical significance.

Evaluation of the natural evaporation was attempted by the use of simple soil evaporimeters, the technique used being similar to that employed by Pasquill (1949*a*), who provided a justification for the method when used on clayland pasture in certain conditions. The soil structure on the present site consisted of a gravel loam to a depth of 16 to 18 in., and below this was a layer of gault clay. The soil moisture content was seen to vary considerably from place to place when the surface layers were removed in placing the drag plates in position. The variation in water content with depth was determined at the start and at various times throughout the period of the second series of observations, and found to decrease with depth in every case, which suggested that a soil core isolated at a depth of some inches from lower layers would not show a smaller water loss than the natural surface, at any rate for some time after extraction. To provide some support for this a preliminary experiment was conducted in which six evaporimeters, type A, having a depth and diameter of 4 in., and six, type B, having a depth of 8 in. and a diameter of $2\frac{3}{8}$ in., were exposed at random over the site and the water loss from each measured over three separate periods of an hour. The twelve evaporimeters were set out in about 90 min, and a fresh selection of cores were inserted for each hour's readings. The results are shown in table 1 and indicate the scatter that was always present in the performance of the evaporimeters due to the heterogeneous nature of the soil-particle size, and therefore water content. There is, however, no systematic effect due to core depth. Since the type A evaporimeters were more convenient, these were used in the general programme of observations, and the rates of evaporation given in table 3 are the mean indication from six for which new cores were cut and inserted on every day of observation to eliminate, as far as possible, any influence of core age and consistent errors due to non-representative selection of samples on any one day. During a few observations condensation at the surface was observed. To what extent the evaporimeters provide a satisfactory measure of dew-fall cannot be ascertained. We may note that the results in such cases are in keeping with the general run and there seems to be no reason for rejecting them out of hand. In a few observations the rate of evaporation was very small and no value has been given.

Table 1. Relative water losses from type A and type B evaporimeters expressed as percentages of the loss from one type A evaporimeter

16 Sept. 1952	type A							type B						
time (G.M.T.)	1	2	3	4	5	6	mean	1	2	3	4	5	6	mean
11.00 to 12.00	100	62	112	105	77	93	92	87	132	96	90	77	50	89
14.00 to 15.00	100	137	93	67	99	113	102	109	97	127	96	103	129	110
17.00 to 18.00	100	147	107	184	141	131	135	173	81	156	98	131	81	120

The flux of heat in the ground was obtained by the use of a thermo-electric thermometer having bulbs at 0, $\frac{1}{2}$, 1, 2, 4, 6, 8, 12 and 16 in. below the surface. The temperature at each depth was read at the start and finish of each observation, and it is assumed that the temperature change was linear with time. A further requirement was a knowledge of the specific heat of the soil material. At the start of the second series of observations soil cores were taken in three places and the specific heat of the material, after drying, was determined by the method of mixtures. There was no systematic variation with depth down to 8 in. and the value 0·20 was obtained and used. On each day of heat-balance observation three more cores were taken and the water content found in the layers 0 to 1, 1 to 2, 2 to 4 and 4 to 8 in., and the actual specific heat in each layer calculated. A detailed account of the procedure is given by Pasquill (1949 *a*). A Moll solarimeter calibrated at Kew Observatory was used to measure the short-wave radiative flux. From time to time it was inverted

Table 2. Observed wind speeds, air temperatures and surface drags together with reduced data for observations nos. 1 to 26

observation no.	...	1	2	3	4	5	6	7	8	9	10	11	12	13	14	15	16	17	18	19	20	21	22	23	24	25	26
date (1952)	...	7.7	7.7	7.7	8.7	8.7	8.7	9.7	16.7	17.7	17.7	12.8	12.8	12.8	13.8	13.8	14.8	14.8	15.8	15.8	15.8	15.8	15.8	29.8	29.8	29.8	1.9
midtime of observation (G.M.T.)	...	14.15	15.10	16.00	14.45	15.30	16.15	13.20	14.20	12.35	15.15	14.30	13.30	14.30	14.07	10.52	15.55	16.00	10.55	11.45	13.15	14.00	15.30	11.45	13.55	14.45	11.15
wind speed, u (cm/s) at z cm	200	594	550	658	487	417	417	241	622	356	387	800	853	915	615	627	182	152	427	438	560	568	536	213	184	148	664
	150	576	540	634	472	405	407	233	592	344	369	766	830	900	589	599	173	147	411	419	546	547	511	208	181	143	639
	100	543	521	602	451	387	388	223	570	328	356	731	801	855	564	576	168	138	393	402	525	522	482	201	174	139	603
	75	521	504	585	418	359	366	216	547	314	331	669	749	822	542	546	161	139	377	381	503	503	463	194	166	133	576
	50	479	470	543	383	337	344	201	514	290	306	608	688	761	494	502	151	127	340	346	453	462	421	184	161	123	548
	37½	447	440	507	377	317	322	188	484	273	290	561	639	712	467	473	145	122	332	333	441	444	405	176	149	121	506
	25	397	380	442	335	288	296	175	441	247	260	496	561	619	416	421	129	110	280	286	375	382	357	158	137	109	449
	15	332	325	385	311	262	260	159	390	223	234	410	479	515	379	380	117	97	240	245	302	320	302	142	119	98	402
air temperature T (°F) at z cm	200	73·4	73·2	73·5	66·3	68·0	69·6	75·1	67·9	66·7	66·8	72·7	74·9	74·4	74·6	74·4	73·4	73·2	72·8	73·2	73·0	73·4	66·6	69·9	71·4	73·5	65·4
	150	73·48	73·33	73·63	66·35	68·01	69·64	75·17	68·20	66·87	66·87	72·75	75·04	74·51	74·73	74·43	73·38	73·27	72·88	73·16	73·19	73·64	66·62	69·99	71·52	73·67	65·67
	100	73·78	73·68	73·80	66·46	68·18	69·79	75·31	68·62	67·06	66·96	73·04	75·32	74·77	75·00	74·50	73·86	73·42	73·24	73·57	73·76	73·97	66·66	70·35	71·70	73·89	66·08
	50	74·17	74·67	74·35	66·88	68·54	70·22	75·71	69·35	67·39	67·12	73·54	75·84	75·11	75·70	74·71	74·46	73·63	73·91	73·69	74·41	74·51	66·73	71·15	72·32	74·47	66·75
	37½	74·36	75·01	74·42	67·01	68·56	70·43	75·88	69·68	67·57	67·20	73·83	75·99	75·32	76·12	74·87	74·93	73·80	74·24	73·84	74·74	74·78	66·76	71·69	72·68	74·74	67·04
	25	74·77	75·74	75·15	67·41	69·06	70·70	76·10	70·28	68·01	67·44	74·21	76·35	75·53	76·71	75·10	75·62	74·07	74·64	73·93	75·28	75·22	66·79	72·37	73·25	75·20	67·50
$10^2 \frac{\partial u}{\partial z}$ (sec^{-1})	150	47	29	43	29	31	23	15	52	33	48	66	63	59	36	51	14	12	31	33	52	43	41	8	8	9	61
	75	123	104	129	115	92	89	49	106	70	87	227	198	178	121	121	27	24	90	105	122	123	113	33	32	30	131
	37½	347	287	319	233	220	187	101	269	175	161	476	481	567	336	301	88	68	209	202	284	249	240	84	87	63	264
$-10^4 \frac{\partial T}{\partial z}$ (°C cm^{-1})	150	17	26	17	11	13	12	13	37	17	11	17	17	14	22	9	39	13	25	11	35	24	—	21	16	19	37
	75	45	95	51	41	39	47	41	76	37	20	59	56	42	75	22	73	27	72	33	94	69	9	92	66	64	79
	37½	127	261	127	83	93	98	84	193	93	37	123	137	134	209	54	249	74	165	64	192	140	19	233	178	134	158
$-10^3 R$	150	27	106	32	48	49	82	206	47	57	17	14	15	14	59	13	677	322	90	37	44	45	—	1147	883	818	34
	75	10	29	10	11	16	20	58	23	26	9	4	5	4	17	5	336	161	30	10	21	15	3	285	218	239	16
	37½	4	11	4	5	6	9	27	9	10	5	2	2	1	6	2	107	54	13	5	8	8	1	110	79	112	8
τ_0 (dynes cm^{-2})	—	2·35	2·01	2·97	1·39	1·14	1·10	0·379	2·33	0·858	0·607	3·73	3·81	3·04	2·47	1·96	—	0·253	0·651	0·809	1·50	1·43	1·63	0·408	0·406	0·375	1·74
$10^2 \tau_0 \Big/ \rho z^2 \left(\frac{\partial u}{\partial z}\right)^2_z$	150	39	89	59	62	44	77	62	32	29	10	31	36	32	67	28	—	65	25	27	14	29	36	237	235	171	17
	75	23	28	27	16	20	21	23	31	26	12	10	29	14	25	20	—	65	14	11	15	14	19	71	59	63	15
	37½	11	14	17	15	14	19	22	19	16	14	10	10	5	13	13	—	32	10	12	10	13	16	34	32	60	15
$10^3 C_D$ referred to u_{200}	—	11·1	11·1	11·4	9·8	10·9	10·5	10·9	10·0	11·3	6·8	9·7	8·7	6·1	10·9	8·3	—	18·3	6·0	7·0	8·0	7·4	9·5	15·0	20·0	28·5	6·6

TABLE 3. OBSERVATIONS OF WIND SPEEDS, AIR TEMPERATURES AND HUMIDITIES, SURFACE DRAGS, AND RATES OF EVAPORATION TOGETHER WITH REDUCED DATA FOR OBSERVATIONS NOS. 27 TO 51

observation no. ...		27	28	29	30	31	32	33	34	35	36	37	38	39	40	41	42	43	44	45	46	47	48	49	50	51
date (1952) ...		8.10	8.10	8.10	8.10	10.10	10.10	15.10	15.10	16.10	16.10	17.10	17.10	17.10	17.10	17.10	17.10	17.10	24.10	24.10	24.10	7.11	7.11	7.11	7.11	7.11
midtime of observation (G.M.T.) ...		14.45	16.45	19.15	21.45	11.00	13.15	14.10	15.00	11.18	14.00	14.15	15.30	16.55	18.30	19.30	20.30	21.30	18.15	20.00	21.00	17.15	18.15	19.15	20.15	21.15
wind speed, u (cm/s) at z cm	200	437	608	238	393	374	368	215	235	157	199	369	339	254	126	70	108	66	577	591	657	326	264	249	307	342
	150	409	571	216	368	360	355	205	223	152	192	352	326	236	115	64	96	62	549	563	624	310	250	239	292	328
	100	379	525	194	333	341	337	194	207	143	181	330	302	216	101	51	81	54	506	518	575	291	232	222	272	305
	75	362	508	182	325	327	327	186	194	135	173	316	284	208	99	50	74	49	490	511	562	273	214	209	253	284
	50	336	463	164	292	307	302	173	184	130	159	288	263	186	81	41	61	44	442	453	504	252	197	193	232	262
	$37\frac{1}{2}$	320	449	154	279	292	286	166	174	125	150	273	250	180	78	37	56	41	427	438	490	239	187	179	221	251
	25	272	405	140	260	267	262	148	157	117	141	254	231	165	71	33	50	35	390	407	462	216	168	160	197	223
	15	250	352	121	225	237	230	134	136	102	124	223	203	144	59	—	41	30	352	364	428	190	146	142	172	166
air temperature T (°F) at z cm	200	54·0	54·1	46·3	46·0	49·1	51·3	51·0	51·6	47·7	51·6	55·2	55·6	54·3	53·2	45·4	43·9	43·3	47·3	47·4	48·1	42·5	40·1	39·0	39·5	40·2
	150	54·01	54·01	45·98	45·84	49·25	51·36	51·03	51·62	47·79	51·61	55·26	55·60	54·19	53·07	45·24	43·66	43·10	47·18	47·29	47·98	42·41	39·94	38·88	39·39	40·09
	100	54·01	53·91	45·64	45·63	49·48	51·52	51·15	51·63	48·05	51·67	55·47	55·64	54·05	52·91	44·99	43·43	42·82	47·11	47·10	47·76	42·18	39·66	38·69	39·23	39·92
	50	54·03	53·74	45·18	45·26	50·01	51·83	51·37	51·63	48·38	51·74	55·71	55·65	53·81	52·67	44·60	43·00	42·29	46·71	46·82	47·42	41·76	39·18	38·43	38·78	39·59
	$37\frac{1}{2}$	54·03	53·68	45·02	45·13	50·26	51·93	51·62	51·71	48·66	51·78	55·93	55·78	53·73	52·58	44·41	42·87	41·94	46·60	46·72	47·32	41·53	39·00	38·28	38·64	39·38
	25	54·07	53·60	44·77	44·93	50·64	52·18	51·80	51·73	48·92	51·84	56·21	55·84	53·55	52·43	44·07	42·60	41·32	46·40	46·49	47·07	41·18	38·69	38·10	38·37	39·23
absolute humidity χ (g m^{-3}) at z cm	200	7·34	7·31	6·91	6·62	5·64	5·44	6·07	6·40	6·48	5·68	6·94	6·77	6·81	7·04	6·46	6·32	6·19	6·87	6·89	6·75	4·91	5·02	6·27	5·31	5·15
	150	7·36	7·33	6·89	6·62	5·68	5·47	6·03	6·47	6·50	5·69	6·95	6·78	6·81	7·09	6·44	6·28	6·18	6·89	6·89	6·76	4·91	5·02	6·28	5·29	5·15
	100	7·38	7·36	6·84	6·63	5·81	5·49	6·18	6·56	6·49	5·74	6·98	6·82	6·96	7·16	6·43	6·26	6·15	6·88	6·90	6·78	4·91	5·02	6·30	5·31	5·16
	50	7·51	7·45	6·82	6·65	6·00	5·65	6·33	6·77	6·66	5·90	7·14	6·95	6·97	7·28	6·40	6·24	6·09	6·95	6·92	6·83	4·92	5·03	6·31	5·30	5·19
	$37\frac{1}{2}$	7·60	7·51	6·82	6·67	6·11	5·75	6·36	6·81	6·77	6·02	7·33	7·07	7·05	7·34	6·39	6·21	6·07	6·95	6·93	6·85	4·96	5·05	6·32	5·30	5·21
	25	7·73	7·63	6·80	6·69	6·32	5·94	6·64	6·85	6·90	6·19	7·49	7·34	7·11	7·41	6·38	6·21	6·00	7·00	6·98	6·88	4·99	5·07	6·33	5·30	5·27
$10^2 \frac{\partial u}{\partial z}$ (sec^{-1})	150	53	71	44	51	31	26	17	25	13	14	31	37	30	18	15	25	—	50	62	74	25	28	29	33	33
	75	83	134	62	87	64	60	39	44	27	41	71	78	57	37	25	37	19	130	128	130	71	57	53	81	85
	$37\frac{1}{2}$	202	232	88	151	157	171	102	99	65	97	179	144	123	62	48	65	48	225	214	212	162	102	120	133	159
$10^4 \frac{\partial T}{\partial z}$ (°C cm^{-1})	150	—	10	37	23	−26	−12	−11	—	−18	—	−14	—	13	13	25	28	27	14	16	21	16	25	16	19	16
	75	—	19	52	39	−53	−28	−26	—	−39	−9	−32	−8	26	28	43	43	57	37	32	36	47	51	29	47	40
	$37\frac{1}{2}$	−4	33	74	69	−130	−81	−67	−8	−93	−22	−80	−15	55	47	82	74	139	64	53	59	106	90	67	78	75
$10^{10} \frac{\partial \chi}{\partial z}$ (g cm^{-4})	150	—	−10	—	—	−19	−11	−14	−16	−11	−11	—	−15	−12	−12	—	—	—	—	—	—	—	—	—	—	—
	75	−26	−20	—	—	−39	−25	−32	−27	−25	−32	−32	−30	−23	−25	—	—	11	−10	—	−8	—	—	—	—	—
	$37\frac{1}{2}$	−82	−34	10	−15	−95	−72	−82	−61	−58	−76	−122	−56	−50	−42	9	11	26	−17	−7	−13	−27	−17	—	—	−12
$10^3 R$	150	—	6	65	30	−98	−66	−144	—	−392	—	−54	—	46	128	373	152	—	18	14	13	84	108	63	59	49
	75	—	3	46	14	−45	−29	−61	—	−191	−21	−22	−5	26	107	235	108	546	7	7	7	32	55	35	25	19
	$37\frac{1}{2}$	0	2	33	10	−18	−10	−23	−3	−77	−11	−9	−3	12	41	123	61	211	4	4	4	14	30	16	16	10
τ_0 (dynes cm^{-2})	—	1·22	1·11	0·296	0·982	1·04	0·850	0·342	0·373	—	—	0·762	0·520	0·308	0·080	0·026	0·085	0·028	1·54	2·23	2·59	—	0·191	0·244	0·457	0·403
$10^2 \tau_0 / \rho z^2 \left(\frac{\partial u}{\partial z}\right)^2_z$	150	16	8	6	13	41	47	44	22	—	—	30	14	24	9	4	4	—	23	21	12	—	9	11	15	13
	75	26	10	11	19	37	35	33	29	—	—	22	12	14	9	6	8	12	14	26	23	—	9	13	10	8
	$37\frac{1}{2}$	18	13	22	26	25	17	20	22	—	—	14	15	6	10	7	12	7	18	29	34	—	11	10	15	9
$10^8 E_0$ (g cm^{-2} sec^{-1})	—	348	205	−28	51	567	322	315	257	233	200	355	245	105	38	—	—	−16	165	24	165	60	43	−75	−26	24
$-E_0 / z^2 \left(\frac{\partial u}{\partial z}\right)_z \left(\frac{\partial \chi}{\partial z}\right)_z$	150	—	13	—	—	43	50	60	29	72	58	—	20	15	18	—	—	—	—	—	—	—	—	—	—	—
	75	29	14	—	—	40	38	45	38	61	27	28	19	15	7	—	—	14	23	—	11	—	—	—	—	—
	$37\frac{1}{2}$	15	19	22	15	27	19	27	30	44	19	12	28	15	10	—	—	9	31	12	17	12	15	—	—	9
Kv_{75} (cm^2 sec^{-1})	—	1340	1020	—	—	1450	1290	980	950	930	620	1110	820	460	150	—	—	150	1650	—	2060	—	—	—	—	—
Km_{75} (cm^2 sec^{-1})	—	1230	690	400	940	1360	1180	730	710	—	—	900	560	450	180	90	190	120	990	1740	1670	—	280	370	470	390
$10^3 C_D$ referred to u_{200}	—	10·6	5·0	8·7	10·6	12·4	10·5	12·3	11·3	—	—	9·3	7·5	8·0	8·4	8·8	12·1	10·7	7·7	10·6	10·0	—	4·6	6·6	8·1	5·7

Table 4. Observed heat-balance components and values of the three diffusivities

observation no. ...	29	30	31	33	35	44	45	46	47	48	50
heat components (cal cm^{-2} min^{-1})											
net incoming solar radiation	—	—	0·568	0·329	0·459	—	—	—	—	—	—
net outward long-wave radiation at 75 cm	0·104	0·102	0·168	0·142	0·144	0·122	0·122	0·118	0·119	0·116	0·115
heat gained by soil	−0·043	−0·024	0·046	0·015	0·043	−0·055	−0·024	−0·035	−0·030	−0·082	−0·056
heat used in evaporation	−0·010	0·018	0·204	0·114	0·084	0·059	0·009	0·059	0·022	0·015	−0·009
heat associated with turbulent transport	−0·051	−0·096	0·150	0·058	0·188	−0·126	−0·107	−0·142	−0·111	−0·049	−0·050
Kh_{75} (cm^2 sec^{-1})	560	1400	1540	1190	2610	1940	1920	2250	1340	590	600
Kv_{75} (cm^2 sec^{-1}) (from table 3)	—	—	1450	980	930	1650	—	2060	—	—	—
Km_{75} (cm^2 sec^{-1}) (from table 3)	400	940	1360	730	—	990	1740	1670	—	280	470

to obtain a measure of the percentage of incident radiation reflected at the surface. The long-wave, atmospheric, radiation from ground and sky was estimated by the method described by Robinson (1947), the only observation required on the site in addition to the temperature and humidity profiles being the reading of a spirit-in-glass thermometer resting on the ground. In constructing the curve of water content against temperature on the radiation chart temperatures and humidities above 2 m were taken from the result of radiosonde ascents at Larkhill and Hemsby.

The observational data for both series of observations are set out in tables 2, 3 and 4, together with various reduced data which will be referred to later.

3. The profiles and gradients of wind, temperature and humidity

In the computations which follow the vertical gradients of the elements are required. Pasquill (1949*a*) in deriving gradients for the majority of his observations, assigned the same functional form to the three profiles and obtained his gradients arithmetically, whereas Rider & Robinson (1951) preferred to make no assumption as to the form of the profiles and obtained gradients by tangent drawing to the best freehand curves that could be constructed through the measured values when the latter were plotted against a linear height scale. These latter investigators concluded that in the majority of cases the ratios of the gradients of any two of the elements were approximately constant with height, and this led them to plot the measured values of the elements on one curve after the scales had been adjusted so that the best freehand profiles coincided at two heights. They were able to show that for the majority of their observations the profiles had the same form. In the present work the measured values of the elements were plotted against a linear height scale and the best curves drawn through the plots. The scales were then adjusted so that the profiles drawn by hand coincided at 37·5 and 150 cm, and the temperature, humidity and wind profiles were then plotted on one curve using the appropriate scales. In the first series it was found that for every observation one curve could be constructed to represent the most likely profile of both wind and temperature. Figure 4 shows the superposed plots for observations 14 and 19, the first a typical example, the second the worst in the series. In the second series of observations it was found that the three elements could be represented by one curve in nineteen of the twenty-five cases. In five observations (nos. 27, 30, 37, 47 and 48) the humidity profile appeared to have a different functional form and could not be represented by the same curve as the wind and temperature. However, it must be noted that in only one of these five cases (no. 37) did the individual humidity points show a departure from the superposed wind and temperature profile which was outside the accuracy expected in the humidity measurements. Nevertheless the departures were systematic in all these five observations. Figure 5 shows a typical example in observation 30 and a plot for observation 37. Two examples in which one curve was drawn to represent the three elements are illustrated in figure 6. In observation 50 the humidity profile was vertical within the limits of measurement. The observations were made in all conditions of wind speed, temperature, sky, etc., and it appears permissible to conclude that the wind and temperature profiles

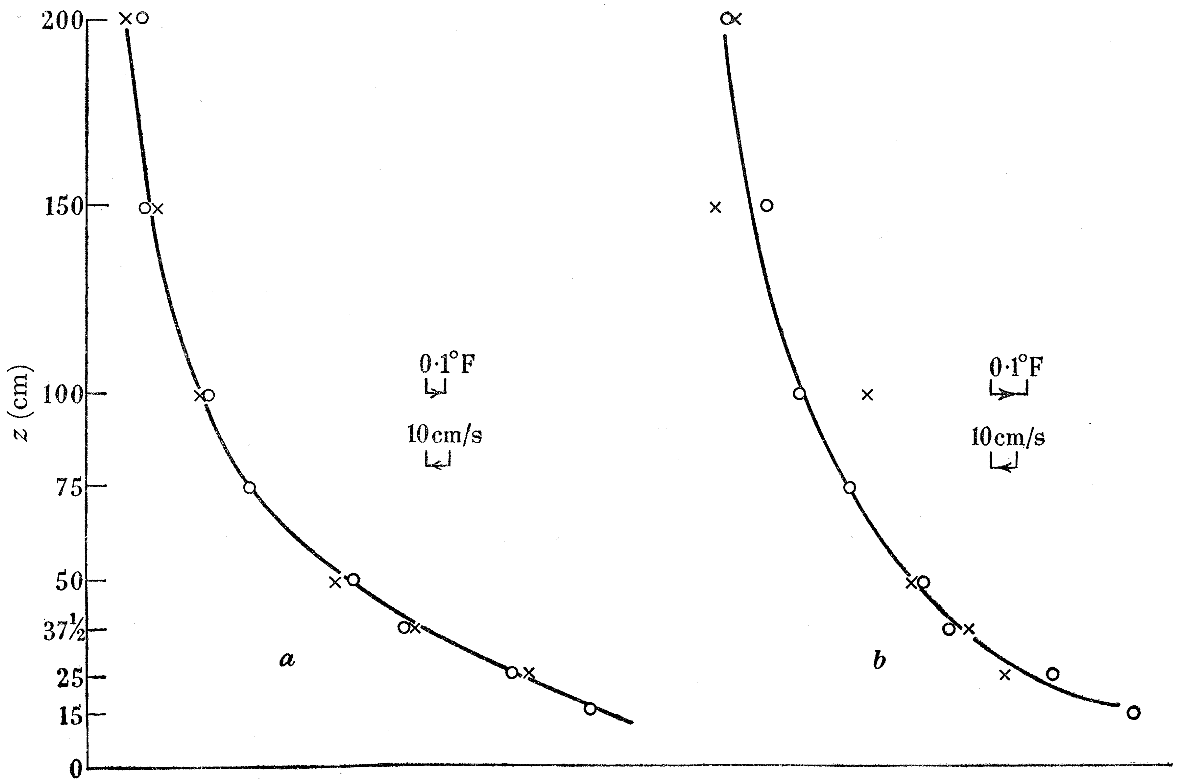

FIGURE 4. Examples of superposed wind and temperature profiles: curve *a*, observation 14; curve *b*, observation 19; ○, wind; ×, temperature.

have the same functional form and that this form is shared by the humidity profile on most occasions. The exceptions that occur in the humidity profile do not appear to be associated with any particular conditions.

The vertical gradients of wind $\partial u/\partial z$ and temperature $\partial T/\partial z$ which appear in table 2 were measured from tangents drawn to the superposed profiles. The gradients which appear in table 3 have been obtained in the same way for the wind and temperature and humidity $\partial \chi/\partial z$ where possible, but in those cases where the humidity profile could not be considered to be represented by the same curve as the wind and temperature the humidity gradients were found from the best curve that could be constructed through the humidity points alone. The temperature and humidity gradients are given to 1×10^{-4} °C cm^{-1} and 1×10^{-10} g cm^{-4} respectively, and in general gradients of magnitude less than ten times these values have been omitted as unreliable. The reliability of gradients obtained in this way has often been questioned, and an attempt was made to assess the degree to which the freehand profiles

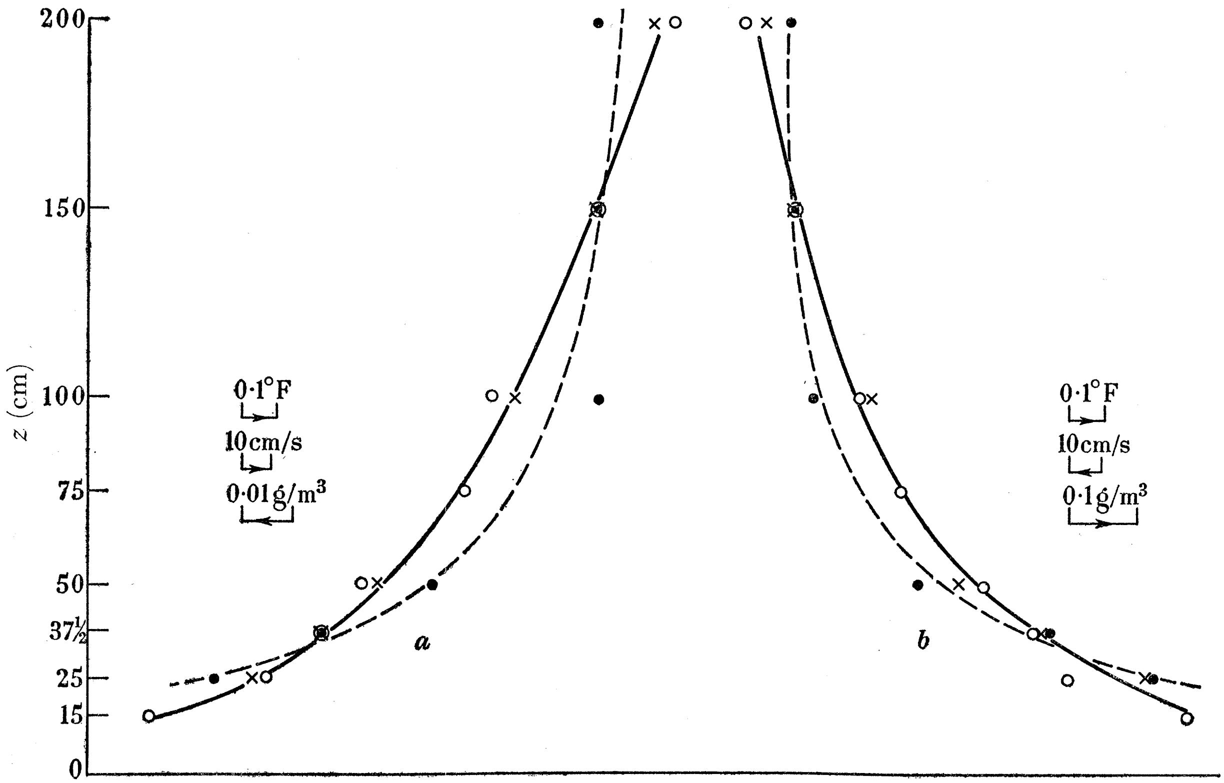

FIGURE 5. Superposed plots of wind, temperature and humidity: curves *a*, observation 30; curves *b*, observation 37; —, common wind and temperature profiles; – – –, humidity profiles; ○, wind; ×, temperature; ●, humidity.

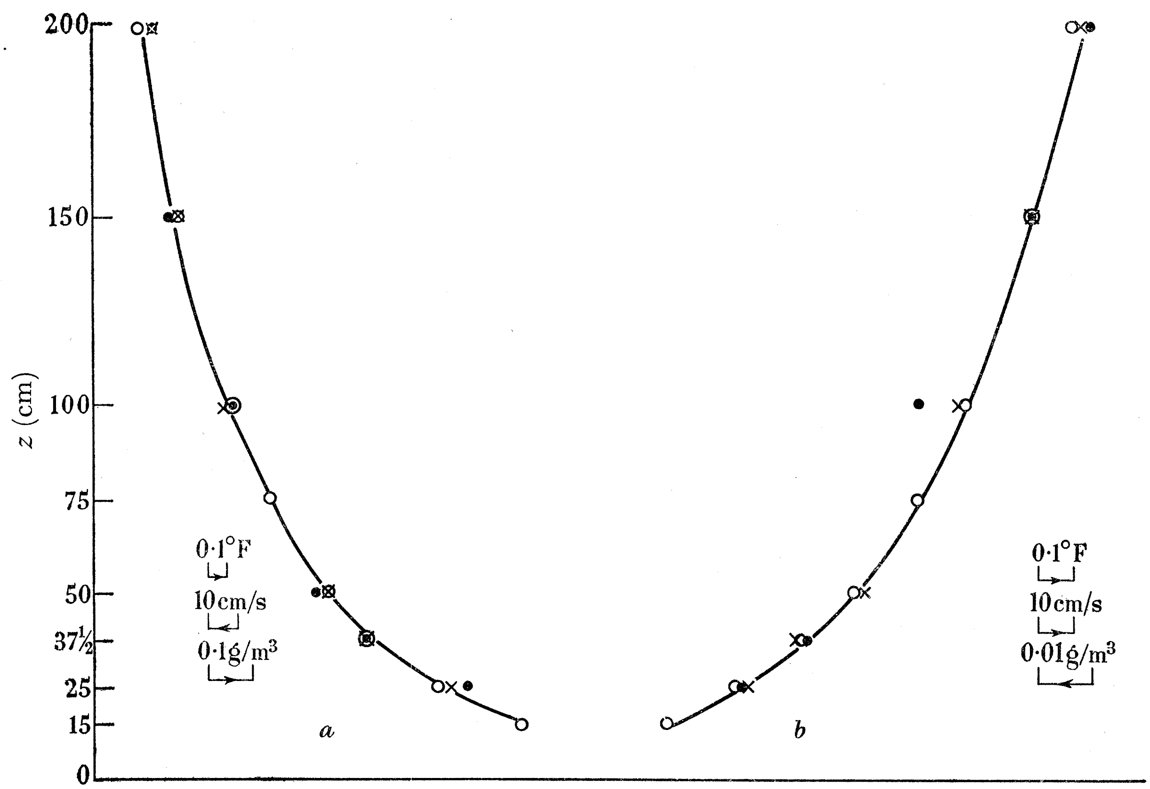

FIGURE 6. Examples of superposed wind, temperature and humidity profiles: curve *a*, observation 31; curve *b*, observation 49; ○, wind; ×, temperature; ●, humidity.

PHILOSOPHICAL TRANSACTIONS OF THE ROYAL SOCIETY A MATHEMATICAL, PHYSICAL & ENGINEERING SCIENCES

and gradients can be reproduced. After the observations had been treated as described, observation 14 was chosen and three observers independently found the gradients, as has been described. The results for the temperature gradients are given in table 5. (The wind gradients differ from the temperature gradients by a constant factor.) This suggests that the gradients given are reliable to 10%. It must be noted that the major part of the uncertainty is introduced in the construction of the profiles rather than in the construction of the tangents to a given profile. In the arithmetical method used by Pasquill (1949*a*) errors in the temperature measurements of the order of 0·02° C would give errors in the deduced gradients comparable to the uncertainty in the method used here.

TABLE 5. GRADIENT DETERMINATIONS BY THREE OBSERVERS

$10^{-4}\left(\frac{\partial T}{\partial z}\right)$ (° C cm^{-1}) at z cm for observation No. 14

observer	$z=150$	$z=75$	$z=37{\cdot}5$
E. L. E.	22	76	187
P. H. L.	17	71	197
N. E. R.	21	82	196
means	20 ± 2	76 ± 4	194 ± 6
original determination by N. E. R. as in table 2	22	75	209

From a long series of wind-profile observations Deacon (1949, 1953) proposed the generalized wind-profile law

$$\frac{\partial u}{\partial z}=az^{-\beta}, \tag{1}$$

where β takes values <1, $=1$ and >1, in stable, neutral and unstable conditions, respectively. Since the form of the temperature profile is the same as that of the wind profile a similar law should hold for temperature. The same functional form is followed by the humidity profile on the majority of occasions. Work by Deacon and others has resulted in the recognition that the form of the profile of wind speed is controlled by the magnitude of the wind speed as well as by the temperature gradient. This is to be expected, since the wind speed is a measure of the shearing force which opposes any modification of the pattern of air flow due to buoyancy forces. The so-called Richardson number, R, defined by

$$R=\frac{g\left(\frac{\partial T}{\partial z}+\Gamma\right)}{T\left(\frac{\partial u}{\partial z}\right)^2},$$

where g is the gravitational acceleration, T is the absolute temperature and Γ is the dry adiabatic lapse rate (-1×10^{-4} ° C cm^{-1}), which has proved to be a convenient indicator of the state of the atmosphere for this purpose, has been calculated for the three heights 37·5, 75 and 150 cm where possible and inserted in tables 2 and 3. A method often used for the study of the shape of the profiles is to plot values of the parameter

$$\frac{A_1-A_z}{A_1-A_2},$$

where A_z represents the wind speed, temperature or humidity as desired at height z, A_1 and A_2 being the values at two fixed heights, against the height on a logarithmic scale. On investigating the present measurements in this way it was found that, in general, the plots of A against $\log z$ were concave to the $\log z$-axis in unstable conditions, convex to it in stable conditions, and showed an approximately linear variation with $\log z$ in near neutral conditions. Exceptions occurred which are thought likely to be due to experimental errors in the observed magnitude of $(A_1 - A_2)$ which has a large influence on the shape of the plot.

4. The eddy diffusivity for momentum

In specifying the eddy diffusivity for momentum at the height z, Km_z, it has been the custom (see, for example, Calder 1949) to employ the well-established laboratory law relating the drag exerted on an artificially roughened surface to the fluid velocity at a height z above the surface, u_z, in turbulent flow, namely,

$$u_z = \frac{1}{k}\left(\frac{\tau_0}{\rho}\right)^{\frac{1}{2}} \ln\left(\frac{z}{z_0}\right), \tag{2}$$

where k is a constant having the value 0·40, τ_0 is the drag on the surface, ρ is the density of the air which will be given the value $1{\cdot}2 \times 10^{-3}\,\mathrm{g\,cm^{-3}}$ here, and z_0 is the roughness parameter of the surface, a length typical of the surface. It is sometimes necessary to replace z by $(z-d)$ in meteorological applications when the height of the roughness elements is comparable to z, which is measured from the solid air earth interface; d is known as the surface zero displacement. Sheppard (1947) and Pasquill (1950) have shown that the equation holds in the first few metres of the atmosphere in near neutral conditions with values of k approximately equal to the laboratory-determined value. The observations of wind speed and surface drag presented here afford a further opportunity to explore the validity of this equation and to obtain a value for k, von Kármán's constant, and for z_0 which will be required later. Of the fifty-one observations, fourteen were conducted in near neutral conditions as specified by a Richardson number at 75 cm, $R_{75} \leqslant \pm 10 \times 10^{-3}$. The details of these observations have been taken from the main tables and set out in table 6, which contains values of the ratio u_z/u_{75} and of $u_{75}/\tau_0^{\frac{1}{2}}$. Plots of some of the wind ratios show a departure from a smooth u-$\log z$ form, and these arise in part from the difficulty of setting the anemometers relative to one another and to the small departures from neutral conditions. However, a plot of the mean values of the ratio against the height on a logarithmic scale shows a good approach to

Table 6. Wind profile and aerodynamic drag in near neutral conditions

observation no.	10^3R_{75}	u_{75} (cm sec^{-1})	u_z/u_{75} at z cm = 200	150	100	75	50	$37\frac{1}{2}$	25	15	τ_0 (dynes cm^{-2})	$u_{75}/\tau_0^{\frac{1}{2}}$
1	−10	521	1·140	1·106	1·043	1·000	0·919	0·858	0·762	0·637	2·35	341
3	−10	585	1·125	1·084	1·029	—	0·928	0·867	0·756	0·658	2·97	338
10	− 9	331	1·169	1·116	1·077	—	0·925	0·876	0·787	0·707	0·607	424
11	− 4	669	1·196	1·145	1·093	—	0·909	0·839	0·742	0·613	3·73	347
12	− 5	749	1·139	1·108	1·070	—	0·918	0·853	0·749	0·640	3·81	384
13	− 4	822	1·114	1·095	1·040	—	0·926	0·866	0·753	0·627	3·04	472
15	− 5	546	1·149	1·097	1·055	—	0·919	0·866	0·771	0·696	1·96	390
19	−10	381	1·150	1·100	1·055	—	0·908	0·873	0·750	0·643	0·809	423
22	− 3	463	1·157	1·104	1·041	—	0·910	0·875	0·771	0·652	1·63	362
28	+ 3	508	1·197	1·124	1·034	—	0·911	0·884	0·797	0·693	1·11	484
38	− 5	284	1·194	1·148	1·064	—	0·919	0·880	0·838	0·715	0·520	394
44	+ 7	490	1·178	1·120	1·033	—	0·903	0·872	0·796	0·718	1·54	395
45	+ 7	511	1·156	1·101	1·014	—	0·886	0·857	0·796	0·713	2·23	343
46	+ 7	562	1·169	1·110	1·023	—	0·897	0·872	0·822	0·762	2·59	287
means	− 3	—	1·160	1·111	1·048	1·000	0·913	0·868	0·778	0·678	—	385

a straight line with some suggestion of curvature concave to the log z-axis. This latter feature may be the result of the existence of a small zero displacement d due to the grass length, but having regard to the mean value of the Richardson number and to the accuracy of the height setting of the anemometers, the curvature is thought to be insufficient to indicate clearly the need to introduce d in the equation in this case. The u_{15}/u_{75} point would lie on a straight line shown in figure 7 if it were plotted at $z = 14$ cm. The maximum value that could be assigned to d would be about 1 cm, which is small compared with the majority of the heights of wind-speed measurement.

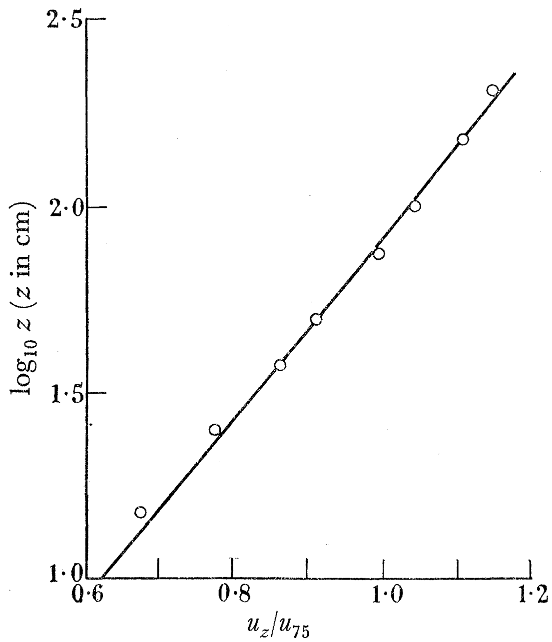

FIGURE 7. Mean velocity profile for the fourteen observations in near neutral conditions.

The equation to the line of figure 4 is

$$u_z/u_{75} = (\log_{10} z + 0{\cdot}49)/2{\cdot}38,$$

which, when compared with equation (2) written in the form

$$\frac{u_z}{u_{75}} = \frac{2{\cdot}303}{ku_{75}}\left(\frac{\tau_0}{\rho}\right)^{\frac{1}{2}}[\log_{10} z - \log_{10} z_0],$$

yields a value of z_0 of 0·32 cm. The mean value of $u_{75}/\tau_0^{\frac{1}{2}}$ is 385, and this in association with the condition

$$\frac{2{\cdot}303}{ku_{75}}\left(\frac{\tau_0}{\rho}\right)^{\frac{1}{2}} = \frac{1}{2{\cdot}38},$$

yields $k = 0{\cdot}41$, which is in good agreement with the laboratory determined value of 0·40.

Now Km_z is defined by

$$Km_z = \frac{-M_z}{\rho\left(\frac{\partial u}{\partial z}\right)_z},$$

where M_z is the vertical flux of momentum at the height z. If it is now assumed that momentum is conserved in the turbulent flow we may replace M_z by τ_0, and this, together with equation (2), leads to the equation

$$Km_z = k^2 z^2 \left(\frac{\partial u}{\partial z}\right)_z. \tag{3}$$

PHILOSOPHICAL TRANSACTIONS OF THE ROYAL SOCIETY A MATHEMATICAL, PHYSICAL & ENGINEERING SCIENCES

A valid method is thus available for the determination of Km in neutral conditions from observations of the wind profile alone.

In stable and unstable conditions this method cannot be used except possibly at small values of z where the departure from neutral conditions and hence from the u-log z form of the profile as indicated by the magnitude of the Richardson number is small on most occasions. In non-neutral conditions generally, Deacon's wind-profile law provides a possible method of specifying Km from wind-profile observations. By integrating equation (1) and employing his observation that the influence of the stability effect on the departure from the u-log z form decreases as the surface is approached, Deacon obtained the equation

$$u_z = \frac{1}{k(1-\beta)}\left(\frac{\tau_0}{\rho}\right)^{\frac{1}{2}}\left[\left(\frac{z}{z_0}\right)^{1-\beta}-1\right], \tag{4}$$

which is analogous to equation (2) and reduces to it for small values of z and for values of β not differing greatly from unity. A difficulty experienced with equation (4) was that the value of z_0 determined from it showed a variation with stability which Deacon considered to be unlikely except perhaps at extreme stability, and he suggested that the apparent variation was probably due to a small variation of β with height. Deacon avoided the difficulty by assuming z_0 to be independent of stability, and that its value was satisfactorily defined by equation (2) and wind-profile observations in neutral conditions. Using the value of z_0 so obtained and wind-profile measurements over the same surface in non-neutral conditions equation (4) was then used to calculate a value for β for the layer concerned. Assuming the validity of equation (4) Km_z is given by

$$Km_z = k^2 z^2 \left(\frac{\partial u}{\partial z}\right)_z \left(\frac{z}{z_0}\right)^{2\beta-2}, \tag{5}$$

or we may write

$$\frac{Km_z}{z^2\left(\dfrac{\partial u}{\partial z}\right)_z} = k^2\left(\frac{z}{z_0}\right)^{2\beta-2},$$

which implies

$$k^2\left(\frac{z}{z_0}\right)^{2\beta-2} = \frac{\tau_0}{\rho z^2\left(\dfrac{\partial u}{\partial z}\right)_z^2}, \tag{6}$$

from the expression defining Km_z.

From our results values of $\tau_0\Big/\rho z^2\left(\dfrac{\partial u}{\partial z}\right)_z^2$ are readily available and have been set out in tables 2 and 3. A number of ways are available for the determination of β, but it is unfortunate that values of this index derived on the basis of single observations of the wind profile are very sensitive to errors in the observations and it is impossible to specify satisfactory values for β from individual observations using the anemometers that were available. We are therefore obliged to use a method in which the observations can be smoothed and this in turn leads to a smooth variation of β with stability. The measured values of $u_{150}/u_{37\cdot5}$ were plotted against the Richardson number at 75 cm. There was some scatter, but a smooth curve could be drawn with some confidence through the points between the limits $10^3 R_{75} = +100$ to -300, and indicated a value of $u_{150/37\cdot5} = 1\cdot285$ at $R_{75} = 0$ which, together with equation (2), gave a value of $z_0 = 0\cdot30$ cm, which has to be compared with the value of 0·32 cm found previously. The degree of agreement is considered to be good as a change of approximately $\pm 0{\cdot}005$ in the value of $u_{150}/u_{37\cdot5}$ is sufficient to change z_0 by $\pm 0{\cdot}02$ cm.

From equation (4) we have
$$\frac{u_{150}}{u_{37\cdot5}} = \frac{(150^{1-\beta}-z_0^{1-\beta})}{(37\cdot5^{1-\beta}-z_0^{1-\beta})},$$
and using the value of 0·30 cm for z_0 the right-hand side of this equation was evaluated for a range of values of β. A curve was thus obtained relating β to R_{75} by using the observed relationship between $u_{150}/u_{37\cdot5}$ and R_{75} and that between $u_{150}/u_{37\cdot5}$ and β. The parameter $k^2\left(\frac{z}{z_0}\right)^{2\beta-2}$ was then evaluated using $k = 0{\cdot}41$ and $z_0 = 0{\cdot}30$ cm for a series of values of β, and finally the values of this parameter were plotted against R_{75}, a plot which is shown as the broken line in figure 8.

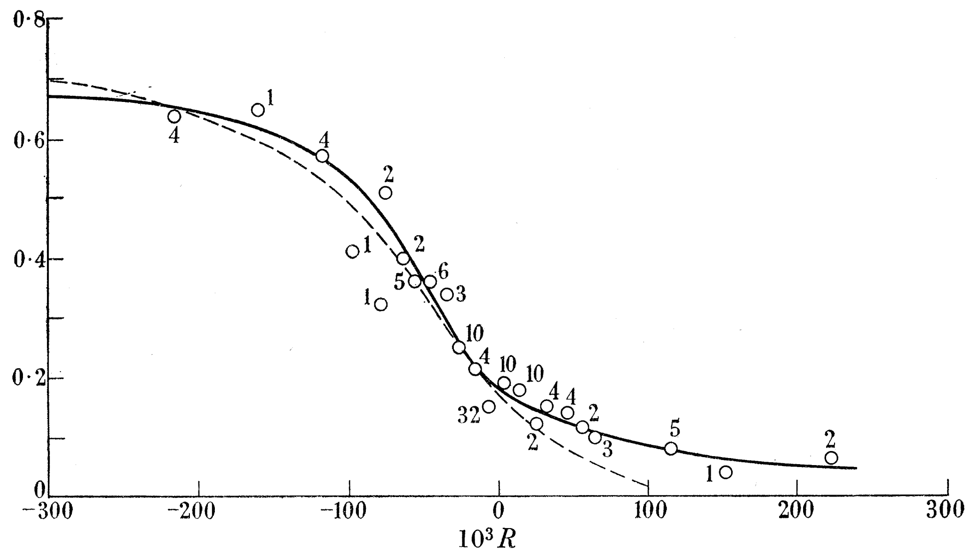

FIGURE 8. Relation between the Richardson number and the observed values of
$$\tau_0\bigg/\rho z^2\left(\frac{\partial u}{\partial z}\right)_z^2 \quad \text{and} \quad k^2\left(\frac{z}{z_0}\right)^{2\beta-2}.$$
○ and —, $\tau_0\bigg/\rho z^2\left(\frac{\partial u}{\partial z}\right)_z^2$; – – –, $k^2\left(\frac{z}{z_0}\right)^{2\beta-2}$.

A plot of the values of the parameter $\tau_0\bigg/\rho z^2\left(\frac{\partial u}{\partial z}\right)_z^2$ against the Richardson numbers at the three heights 150, 75 and 37·5 cm showed some general scatter which arose from the observational inaccuracies, particularly in the determinations of τ_0. There was no separation of the plots according to height, and mean values of the parameter in ranges of Richardson number were calculated and plotted against the mean Richardson number in each range. These plots are shown in figure 8, in which the number attached to each point indicates the number of separate observations represented by the point. A smooth curve was drawn through the plots and is shown as the full line in the figure. In table 7 values of the parameters corresponding to various values of the Richardson number as read from the smooth curves of figure 8 are set out together with other quantities, some of which will be referred to later. It is evident that there is excellent agreement between values of $k^2\left(\dfrac{z}{z_0}\right)^{2\beta-2}$ and $\tau_0\Big/\rho z^2\left(\dfrac{\partial u}{\partial z}\right)_z^2$ in neutral and unstable conditions, but in stable conditions the values of the former parameter become progressively less than those of the latter. The use of equation (5) therefore leads to satisfactory values of Km in unstable (and neutral) conditions, but its use in stable conditions is not permissible and would result in a large underestimation of Km. We may now regard equation (4) as explicitly verified for unstable conditions of flow. By a progressive change in the value of z_0, equation (4) may be made to fit the observations in stable conditions, but it must be noted that this would demand that z_0 should *increase* in magnitude with increasing degree of stability, taking, for example, a value of 1 cm in the region of $R_{75} = +50\times 10^{-3}$. It is difficult to suggest any reason for such a change in z_0; indeed, on intuitive grounds the temptation would be to assign, if anything, a decreasing value to z_0 with the onset and development of stable conditions of flow. We must also note that any likely error in the value of k will not affect the results presented here in any material way.

Table 7

$10^3 R_{75}$	−300	−200	−150	−100	−75	−50	−25	0	+25	+50	+75	+100
$u_{150}/u_{37\cdot 5}$	1·193	1·202	1·206	1·213	1·222	1·235	1·254	1·285	1·321	1·374	1·445	1·548
β (approx.)	1·13	1·12	1·11	1·10	1·08	1·06	1·04	1·00	0·96	0·91	0·85	0·78
$\tau_0\Big/\rho z^2\left(\dfrac{\partial u}{\partial z}\right)_z^2$	0·67	0·64	0·61	0·53	0·46	0·35	0·25	0·17	0·14	0·12	0·10	0·09
$k^2\left(\dfrac{z}{z_0}\right)^{2\beta-2}$	0·70	0·64	0·58	0·49	0·42	0·33	0·25	0·17	0·11	0·07	0·03	0·01
σRM	2·5	3·7	4·8	6·8	8·5	10·4	13·1	—	8·0	8·0	9·1	8·7
σH	10·0	14·0	17·5	21·5	23·2	21·7	19·5	—	6·7	5·7	5·4	4·6
$-E_0\Big/\left(\dfrac{\partial \chi}{\partial z}\right)_z\left(\dfrac{\partial u}{\partial z}\right)_z z^2$	—	0·62	0·60	0·53	0·45	0·37	0·27	0·18	0·16	0·11	0·10	0·08

Another basis on which the results may be examined is provided by the semi-empirical treatments due to Rossby & Montgomery (1935) and Holzman (1943). These treatments lead to the equations:

Rossby & Montgomery:
$$\frac{\tau_0}{\rho z^2\left(\dfrac{\partial u}{\partial z}\right)_z^2} = \frac{k^2}{(1+\sigma R)}; \tag{7}$$

Holzman:
$$\frac{\tau_0}{\rho z^2\left(\dfrac{\partial u}{\partial z}\right)_z^2} = k^2(1-\sigma R). \tag{8}$$

σ is a proportionality factor introduced in the relationship between potential and eddy energy associated with the thermal stratification, the derivation of the equations requiring that σ be constant with respect to stability. Values of σ have been calculated from both equations and are shown in table 7. It will be seen that both equations are unsatisfactory judged by the constancy of σ over the whole range of stability covered, but that the Holzman equation is better than the Rossby-Montgomery equation. In stable conditions only both equations have reasonably constant values of σ, which takes a value of about 8 in equation (7) and of about 6 in equation (8). Either of these equations with the appropriate values

PHILOSOPHICAL TRANSACTIONS OF THE ROYAL SOCIETY A MATHEMATICAL, PHYSICAL & ENGINEERING SCIENCES

of σ would lead to acceptable values of Km in stable conditions and appear superior to Deacon's equation in these circumstances. In table 3 values of Km_{75} which have been calculated from the measured drags and wind-speed gradients have been inserted where possible. The diffusivities lie in the range of magnitude from 10^2 to 10^3.

The surface drag measurements present the opportunity to investigate the dependence of the surface friction coefficient C_D on the magnitude of the wind speed and on the stability. C_D is defined by the equation

$$\tau_0 = \tfrac{1}{2}\rho C_D u_z^2,$$

z being some convenient height near the surface. Tables 2 and 3 contain values of C_D for $z = 200$ cm; a plot of C_D against u_{200} for the fourteen observations in near neutral conditions, those of table 6, shows some scatter but no systematic variation of C_D with wind speed. The mean value of C_D for these observations is 0·0085, which is in general agreement with the values quoted by Sutton (1953). A plot of the values of C_D against the Richardson number shows a marked increase in very unstable conditions, but there is no evidence of a decreased value in stable conditions. The mean value for four very unstable observations (mean R_{75} being $-0{\cdot}226$) is 0·0205, and for four stable observations (mean R_{75} being $+0{\cdot}249$) is 0·010. The change from the near-neutral value probably has no significance in the stable case, but the increase in unstable conditions is not the result of experimental error. Sutton (1953) states that 'variations in C_D cannot be large for any but the largest departures from neutral stability', and this appears to be confirmed by the present results.

5. The eddy diffusivity for vapour

By making the assumption of a negligibly small horizontal variation of absolute humidity, we may obtain values of the eddy diffusivity for vapour at the height z, Kv_z, from the gradients of absolute humidity $\left(\frac{\partial \chi}{\partial z}\right)$ and the rate of evaporation E_0, for by definition

$$Kv_z = \frac{-E_z}{\left(\frac{\partial \chi}{\partial z}\right)_z}, \tag{9}$$

where E_z is the flux of vapour at the height z. We have also

$$E_z - E_0 = -\int_0^z \frac{\partial \chi}{\partial t}\,\mathrm{d}z, \tag{10}$$

and it has been shown previously (for example, Rider & Robinson 1951), and may be further demonstrated from the present results, that the magnitude of the right-hand side of equation (10) is generally small compared with E_0. Even in the worst case in the present observations (no. 43) E_0 is about twenty times the magnitude of the $\int_0^z \frac{\partial \chi}{\partial z}\,\mathrm{d}z$. We may therefore substitute E_0 for E_z in equation (9) with negligible error and write

$$Kv_z = \frac{-E_0}{\left(\frac{\partial \chi}{\partial z}\right)_z},$$

which, in order to facilitate comparison with Km_z arranged in the form

$$\frac{Km_z}{z^2\left(\frac{\partial u}{\partial z}\right)_z} = \frac{\tau_0}{\rho z^2\left(\frac{\partial u}{\partial z}\right)_z^2},$$

we may write as

$$\frac{Kv_z}{z^2\left(\frac{\partial u}{\partial z}\right)_z} = \frac{-E_0}{\left(\frac{\partial \chi}{\partial z}\right)_z\left(\frac{\partial u}{\partial z}\right)_z z^2}. \tag{11}$$

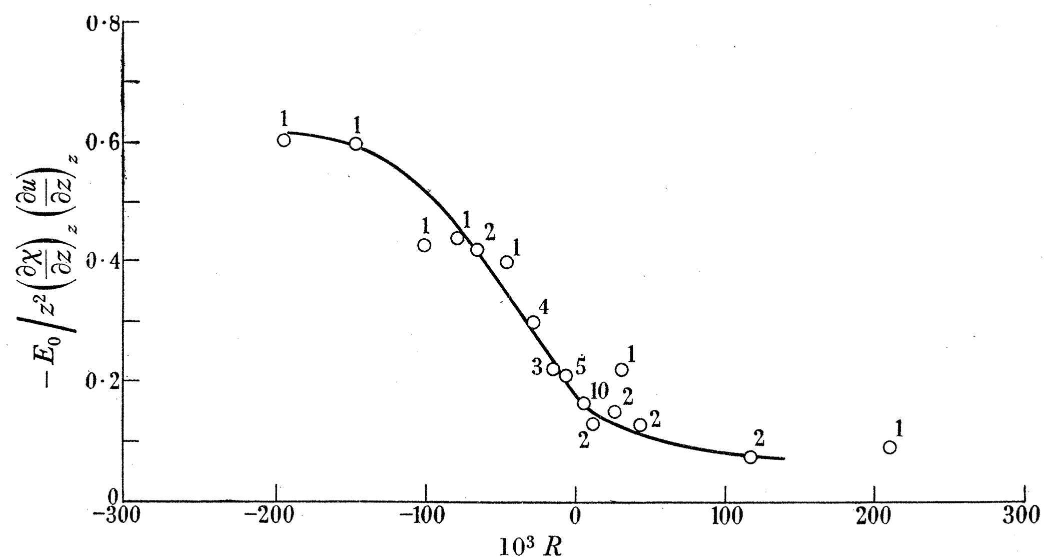

FIGURE 9. Relation between the Richardson number and the observed values of

$$-E_0\Big/z^2\left(\frac{\partial \chi}{\partial z}\right)_z\left(\frac{\partial u}{\partial z}\right)_z.$$

Values of the parameter forming the right-hand side of equation (11) are readily obtained and are set out in table 3. A plot of the parameter against the Richardson number at the three heights 150, 75 and 37·5 shows some scatter but no systematic separation of the plots according to height. In order to aid the construction of a smooth curve through the points, values of the parameter were meaned in ranges of Richardson number and plotted against the mean Richardson number in each range as illustrated in figure 9. Here again the number against each point indicates the number of observations represented by the point. Values of $-E_0\Big/\left(\frac{\partial \chi}{\partial z}\right)_z\left(\frac{\partial u}{\partial z}\right)_z z^2$ corresponding to various values of the Richardson number have been read from the smooth curve drawn on figure 9 and inserted in table 7. It is apparent that throughout the range of stability covered by the observations the values of $-E_0\Big/\left(\frac{\partial \chi}{\partial z}\right)_z\left(\frac{\partial u}{\partial z}\right)_z z^2$ correspond closely with those of $\tau_0\Big/\rho z^2\left(\frac{\partial u}{\partial z}\right)_z^2$. In other words, the equality of the eddy diffusivities for vapour and momentum has been established on a direct observational basis throughout a large range of stability. Pasquill (1949*a*), by assuming the validity of equation (2), was able to show that his observed values of *Kv* in neutral conditions agreed with values of *Km* calculated on the basis of that equation. He also obtained good agreement in unstable but not in stable conditions between values of *Km* and *Kv* when the former were calculated on the assumption of the explicit validity of equation (4). His failure to obtain agreement in stable conditions can be explained by the demonstration in the previous section that satisfactory values of Km are not obtained by the use of equation (4) in stable conditions.

6. The eddy diffusivity for heat

On occasions in the second series of observations when the sky was cloudless and measurement of the net outgoing long-wave radiation was possible, observation of the usual heat-balance components was made with a view to the calculation of the eddy diffusivity for heat, Kh. In the atmosphere near the ground the balance of the heat-exchange process leads to the equation

$$S_0-\left(L_z+\lambda E_0+Q_z+G+\int_0^z C_p\rho\frac{\partial T}{\partial t}\,\mathrm{d}z\right)=0, \tag{12}$$

where S_0 is the net incoming solar radiation at the surface,

L_z is the net outgoing long-wave radiation at the height z,

Q_z is the non-radiative upward flux of heat at the height z,

λE_0 is the heat associated with evaporation, λ being the latent heat of condensation which has been given the value of $600\,\mathrm{cal\,g^{-1}}$, and

G is the heat absorbed in the soil.

The magnitude of the term

$$\int_0^z C_p\rho\frac{\partial T}{\partial t}\,\mathrm{d}z,$$

which is a measure of the heat absorbed in the layer from the ground to the height z, is always small when z is not large and may be neglected in comparison with the other terms of equation (12). By measuring the terms other than Q_z we may obtain a value for the latter and hence a value of Kh_z since, by definition,

$$Kh_z=\frac{-Q_z}{\rho C_p\left(\dfrac{\partial T}{\partial z}+\Gamma\right)}.$$

In this equation C_p, the specific heat of air at constant pressure, has been given the value of 0·25, and ρ, the density of air, has been taken as $1{\cdot}2\times10^{-3}\,\mathrm{g\,cm^{-3}}$.

There were eleven occasions on which L_z could be estimated with confidence using Robinson's (1947) method, and the magnitude of the terms of equation (12) together with the deduced values of Kh_{75} have been set out in table 4 in which values of Km_{75} and Kv_{75} have also been added where they were available. It must be remembered that the values of Km_{75} and Kv_{75} were calculated on the basis of single observations of τ_0 and E_0 respectively and are consequently liable to be considerably in error. Unfortunately, in six of these eleven observations values of Kv_{75} are not available as the humidity gradients were too small to enable values to be given with any confidence. Values of Km_{75} are available in all but two observations, and we are therefore able to compare Kh_{75} with either or both Kv_{75} and Km_{75} in all but one observation, no. 47. While the eddy diffusivity for heat is always greater than the other two diffusivities, the difference is not large on eight occasions when the possible errors, particularly in Km_{75}, are considered. However, in observations 35 and 48, the first a very unstable case, the second a moderately stable case, there is a marked difference between Kh and Km or Kv. In observation 35, Kh_{75} is approximately three times Kv_{75}; in observation 48 it is approximately twice Km_{75}. In neither of these observations are values of both the eddy diffusivities for momentum and vapour available to enable a check of one on the other to be made, but there is no reason to suppose that the values given are grossly in error. It is equally impossible to account for the differences by a likely error in any of the heat balance terms measured. In observation 48 we have an instance where the humidity profile appeared to have a functional form different from that of the wind and temperature profiles, but in observation 35 the profiles of the elements seemed to have a common form. It has been pointed out by Rider & Robinson (1951) that it is very difficult to understand why the diffusivities for heat, vapour and momentum should not be identical when the profiles of the elements have the same form, as this implies that the ratios of the gradients, and hence of the diffusivities themselves, must be constant with height. The observations presented here do not support Pasquill's (1949*a*) result that there is approximate equality between the diffusivities for vapour and heat in stable conditions, but that on passing to unstable conditions the latter becomes progressively greater than the former. Rather, they indicate that for the majority of occasions there is approximate equality irrespective of stability, but that exceptions occur when the diffusivity for heat becomes much larger than that for momentum or vapour. No indication of the proportion of occasions on which this occurs can be given at present.

Acknowledgement is gratefully made to the Director of the Meteorological Office for permission to publish these results. The author is indebted to members of the Meteorological Office Unit at the School of Agriculture for assistance in the observational programme, and to Professor O. G. Sutton, F.R.S., for his interest in the investigation and helpful criticism in the preparation of the paper.

References

Best, A. C. 1935 *Geophys. Mem.* no. 65.
Calder, K. L. 1949 *Quart. J. Mech. Appl. Math.* **2**, pt 2, 153.
Deacon, E. L. 1949 *Quart. J. R. Met. Soc.* **75**, 89.
Deacon, E. L. 1953 *Geophys. Mem.* no. 91.
Holzman, B. 1943 *Ann. N.Y. Acad. Sci.* **44**, 13.
Pasquill, F. 1949*a* *Proc. Roy. Soc.* A, **198**, 116.
Pasquill, F. 1949*b* *Quart. J. R. Met. Soc.* **75**, 239.
Pasquill, F. 1950 *Proc. Roy. Soc.* A, **202**, 143.
Rider, N. E. & Robinson, G. D. 1951 *Quart. J. R. Met. Soc.* **77**, 375.
Robinson, G. D. 1947 *Quart. J. R. Met. Soc.* **73**, 127.
Rossby, C. G. & Montgomery, R. B. 1935 *Pap. Phys. Oceanogr.* **3**, no. 3.
Sheppard, P. A. 1940 *J. Sci. Instrum.* **17**, 218.
Sheppard, P. A. 1947 *Proc. Roy. Soc.* A, **188**, 208.
Sutton, O. G. 1953 *Micrometeorology*, 1st ed. London: McGraw-Hill.

PHILOSOPHICAL TRANSACTIONS OF THE ROYAL SOCIETY A MATHEMATICAL, PHYSICAL & ENGINEERING SCIENCES